Front. Chem. Sci. Eng. 2025, 19(5): 35
https://doi.org/10.1007/s11705-025-2536-3

RESEARCH ARTICLE

A kinetic model-based SOFC combined cycle power generation system for waste heat recovery

Yu Zhuang[1], Tong Jin[1], Mengting Song[1], Jian Du (✉)[1], Siwen Gu[2]

1 Institute of Process Systems Engineering, School of Chemical Engineering, Dalian University of Technology, Dalian 116023, China
2 School of Photoelectric Engineering, Changzhou Institute of Technology, Changzhou 213032, China

Abstract Solid oxide fuel cell (SOFC) is an extremely promising technology for sustainable energy conversion and storage through highly efficient electrochemical reaction at high-temperature conditions. The existing studies commonly address the final equilibrium state of the SOFC electrode reactions, giving less consideration to the micro kinetic of electrode reactions. In this paper, a kinetic model-based SOFC combined cycle power generation system is suggested to recover multiple waste heat, which includes a Kalina cycle (KC) as the bottom cycle and a Rankine cycle (RC) as the top cycle. In devneloping the proposed system, a novel kinetic model is presented for SOFC based on the microscopic mechanism of the oxygen reduction. A dynamic stochastic programming model is established to optimize the integrated system sequentially and simultaneously, with maximum power generation taken as the objective, depending on whether the SOFC system and the KC-RC system are simultaneously optimized. In sequential optimization, the output power of SOFC-KC-RC system is 320.56 kW and it is 415.04 kW using simultaneous optimization, achieving a 29.5% increase in power generation. Further comparison with the previous reports obtained by a thermodynamic model, this work leads to a 10.8% increase in power generation, showing the promising power production performance of the developed system.

Keywords solid oxide fuel cell, kinetic model, plug flow reactor, waste heat recovery

1 Introduction

Climate change is becoming a significant issue along with the growth of the world's fossil energy consumption and greenhouse gas emissions. CO_2 has been proven to have a significant impact on climate change, posing a threat to human survival. Therefore, the development of new technologies for efficient utilization of energy is crucial to alleviate environmental issues. Fuel cells use hydrogen as fuel and water as the reaction product, thus greatly reducing carbon emissions. Solid oxide fuel cell (SOFC), as a high-efficiency energy conversion device with fast electrochemical reaction rate and proton transfer, has attracted extensive attention in the field of power generation, which generates electricity without adversely affecting the environment [1,2]. Owing to the high efficiency of energy conversion, SOFC makes a great contribution to reducing the emissions of CO_2.

From the microscale perspective, an indispensable step to design efficient electrodes is to investigate the micro-electrochemical reaction mechanism of the anode and cathode in SOFC at an experimental scale. In the advancement of oxygen reduction electrodes, manganese strontium lanthanum (LSM) and yttrium stabilized zirconia (YSZ) are widely selected as electrode materials [3−5]. Subsequently, scholars improved the electricity performance of the SOFC system with lanthanum strontium cobalt ferrite (LSCF) and cerium dioxide (GDC) as electrode materials [6,7]. Due to the poor ionic conductivity of single-phase LSM and insufficient active area for cathodic catalytic reactions, the YSZ phase can be further introduced to form porous LSM-YSZ composites. Chan et al. [8] proposed a simple reaction mechanism for the LSM-YSZ composite electrode, which only involved absorbing oxygen and combining the adsorbed oxygen atoms and the oxygen vacancies to produce oxygen ions. Pakalapati et al. [9] proposed an alternative reaction mechanism is proposed for the LSM-YSZ composite electrode. This mechanism consists of a two-phase boundary (2PB) in which oxygen ions migrate and diffuse after entering the electrode, and a three-phase boundary (3PB) in which oxygen ions migrate and diffuse

Received November 20, 2024; accepted December 21, 2024;
online March 16, 2025

E-mail: dujian@dlut.edu.cn

without entering the electrode. Yang et al. [10] put forward a similar reaction mechanism. Banerjee [11] proposed three additional comprehensive reaction mechanisms, which incorporate 2PB and 3PB. However, compared with the reaction mechanism postulated by other researchers, the above reaction mechanism fails to incorporate the migration and diffusion of oxygen ions from the electrode to the electrolyte.

Current advances are limited to thermodynamic modeling of the SOFC when integrated with specific industrial-scale chemical processes [12,13], despite significant research into the micro-electrochemical reaction mechanism of the SOFC. Pianko-Oprych et al. [14] developed an SOFC system based on the thermodynamic reaction model while modeling the SOFC system with an oxygen ion-conducting electrolyte. The anode was simulated using the Gibbs reactor while the cathode was simulated using the separator. After establishing the model, it was compared with the data from experiments to verify the accuracy of the model. Veluswamy et al. [15] built and modeled another SOFC system that includes the electrochemical and the methane reforming reactions, but neglected the combustion reaction. Both of these models were still described by thermodynamic models. Milewski et al. [16] developed a thermodynamic model which uses a Gibbs reactor to model the cathode side and a separator for the anode side. The hydrogen ions needed for the electrochemical reaction are taken out by the anode separator and transferred to the cathode. Saebea et al. [17] developed another model for electrochemical reaction based on the hydrogen ion migration to the cathode. The literature uses Gibbs reactors for modeling the anode and cathode, respectively. In this process, the methane reforming and water gas transfer reactions occur on the anode side, while the entire electrochemical reaction takes place on the cathode side. Compared to oxygen-ion conducting electrolyte SOFC systems, proton conducting SOFC systems are more competitive, but are not widely used due to the lack of suitable cathodes [18].

When it further comes to recovering high-temperature waste heat generated by SOFC system, a number of researches have been reported regarding the application of the thermodynamic cycles for recovering the waste heat, given that the SOFC operates at high temperature and contains a significant quantity of waste heat. In this sense, Kalina cycle (KC), Rankine cycle (RC) and Organic Rankine cycle (ORC) have been well-known waste heat recovery technology to convert multi-grade heat into steam and power. Current research on these technologies concentrates on the appropriate selection of working fluid, the effective integration of thermal cycles and background process, and the technical-economic optimization of the whole system. Regarding waste heat recovery of SOFC system, the main focus is on the recovery of waste heat from the component afterburner for power generation through the gas turbine and then the outlet high-temperature exhaust gas drives the thermodynamic cycle to generate higher quality energy. Wang et al. [19] proposed an SOFC-GT-ORC waste heat recovery system to conduct the waste heat-driven composite energy recovery for the green power ships. The waste heat from exhaust gas flow is combined with ORC to achieve power generation. Chitgar and Moghimi [20] proposed a cogeneration system that uses two different low temperature power generation cycles, including the RC and the KC. In this document, the exhaust gas from the burner enters the gas turbine for work production. The high-temperature exhaust gas from the gas turbine preheats the air and fuel, providing heat for the KC. Tera et al. [21] proposed a further integrated system that includes integrating biomass gasification, SOFC, gas turbine, ORC and supercritical CO_2 Brayton cycle. The system was designed to produce hydrogen, heat and power. The waste heat from the high-temperature gas mixture from the reformer is supplied to ORC. The earlier researches did not consider the multi-grade waste heat recovery of the overall SOFC system but regarded recovering the waste heat of the hot steam in component Afterburner as the primary emphasis.

Based on the above considerations, our previous work has put forward a distributed energy system SOFC-KC-RC in order to attain the maximum conversion efficiency from fuel energy to electricity, which combines KC as a bottom cycle and RC as a top cycle to recover multiple waste heat from the entire SOFC system [22]. Further considering the cathode microscale reaction mechanism that has a great impact on power generation performance, the integration of SOFC kinetic modeling with waste heat recovery has not been well investigated in current research, nor has such optimization work been studied. In this work, to overcome the above-mentioned knowledge gap, an upgraded integrated energy system SOFC-KC-RC is put forward to recover multiple waste heat. The innovative system combines the kinetic mechanism of electrode reaction with multi-configuration thermal cycles, to synergistically enhance the total power generation. For this purpose, a dynamic stochastic programming model is developed for sequential and simultaneous optimization of thermal cycle structures and parameters, as well as for the optimal identification of changing energy-use bottlenecks. Additionally, the presented method allows taking advantage of micro-reaction kinetic mechanism and process operating conditions to further enhance energy integration. Moreover, the superiorities of the novel approach also involve the capacity to efficiently cope with variable temperature conditions (unknown intake and output temperatures of driving heat sources) in order to accomplish particular optimization targets. All of these upgrades, along with more efficient mathematical formulations, provide our model sufficient flexibility to greatly increase computing performance and energy-efficiency solutions.

The structure of this paper is organized below. The next section introduces the enhanced SOFC-KC-RC system, which includes a rigorous kinetic modeling SOFC subsystem based on a cathodic microscale reaction mechanism, an RC subsystem and a KC subsystem. Subsequently, in the third section the model is developed for the entire system considering electrochemical reaction calculation and waste heat recovery optimization. The fourth section presents the optimization results and performs sensitivity analysis to identify the key parameters and investigate how they affect the performance improvements. Finally, the primary remarks and conclusion are summarized in Section 5.

2 Description of the enhanced SOFC-KC-RC system

Following our previous work that only considered a simple thermodynamic model for the simulation of a distributed energy system, more kinetic modeling factors are taken into account in this work. In this sense, an upgraded integrated energy system SOFC-KC-RC system is proposed for the total power generation enhancement. The presented system, as shown in Fig. 1, consists of a rigorous kinetic modeling SOFC subsystem based on a cathodic microscale reaction mechanism, an RC subsystem and a KC subsystem. In the SOFC-KC-RC system, a kinetic modeling approach is adopted to optimize the operating parameters (especially the temperature of the outlet gas in the SOFC). As for the multi-temperature partition waste heat produced by the SOFC, a KC subsystem is installed as a bottom cycle for the purpose of recovering the low-grade temperature waste heat, while as a top cycle, an RC subsystem is installed for high-temperature waste heat recovery. The multi-grade waste heat in SOFC subsystem is used to drive KC and RC to generate power. The high- and medium-temperature waste heat is applied to RC, while the low-temperature waste heat and the condenser in RC are both supplied to KC. The specific heat exchange situations should be optimized as a whole and the detailed model is given in Section 3. The three subsystems will be introduced detailedly in the subsequent section. All potential heat exchange for the entire SOFC-KC-RC system is shown in Fig. 1. All heat sources and heat sinks in the SOFC-KC-RC system are listed in Table 1, and all possible heat exchange occurs between the heat sources and the heat sinks.

2.1 SOFC subsystem

From Fig. 1 it can be seen that the presented SOFC subsystem is composed of eight process units, heater1, mixer1, cooler1, pre-reformer, stack, afterburner, mixer2, cooler2 and separator, respectively. Different from our previous work [22], in the component stack of SOFC system, two plug flow reactors (PFR) are used to model the anode and cathode side based on a rigorous kinetics

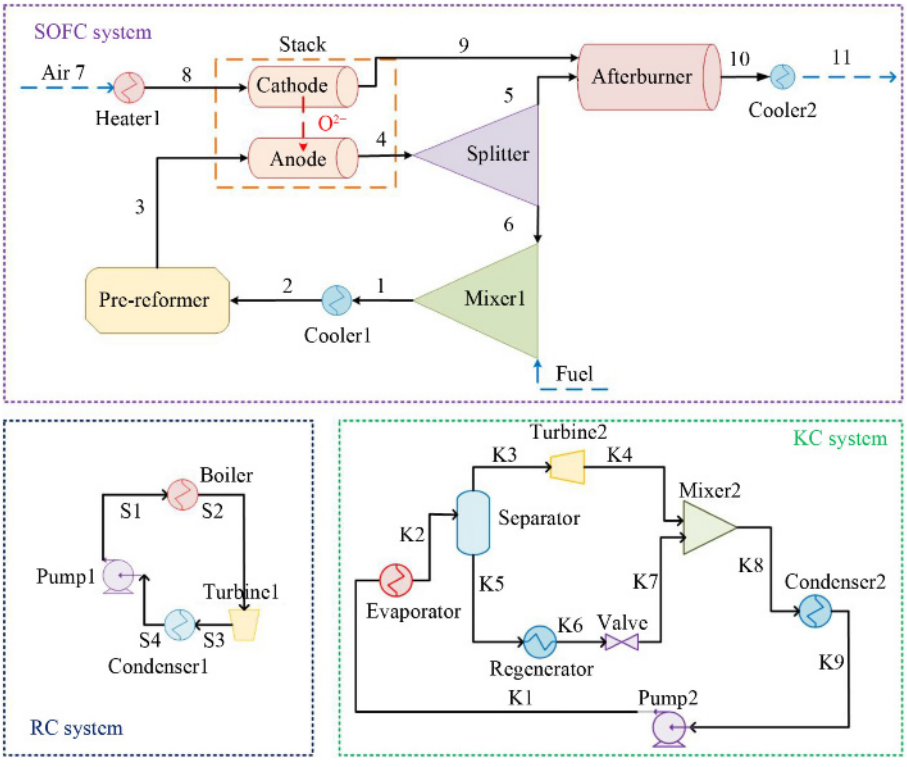

Fig. 1 Schematic diagram of the enhanced SOFC-KC-RC integrated energy system. Reprinted with permission from Ref. [22], copyright 2021, Elsevier.

model (derived from the oxygen reduction reaction mechanism), as shown in Fig. 2.

Figure 2(a) shows the reaction mechanism of the cathode, and Fig. 2(b) illustrates that O^{2-} needs to diffuse through the electrolyte from the cathode side to the anode side in order to react with the fuel in the anode side. It can be seen that the fuel stream is precooled by the cooler1 and then enters the pre-former to conduct a methane reforming reaction. The simulation of the methane reforming reaction is also carried out through a PFR model. The detailed kinetic equations of methane reforming reaction and its corresponding kinetic parameters can be referred to literature [22,23]. The gas from the pre-former then goes to the component stack anode side, while the hot air stream goes to the component stack cathode side. The electrochemical reaction takes place in these two gas streams in the component stack. Part of the gas from the anode of stack is mixed with the fuel stream to undergo methane reforming reaction. Along with the cathode side exhaust gas, the rest of the gas enters the component afterburner for combustion reaction, then cooled by the component cooler2 and discharged.

It should be noted that the simulation of the component stack does not adopt Gibbs reactors and separators. Two PFRs are used to model the cathode and anode sides. According to the rigorous kinetic reaction mechanism, O^{2-} migrates from the cathode to the anode to conduct the electrochemical reaction, as shown in Fig. 2(b). The oxygen reduction reaction mechanism including 2PB and 3PB adopted in the paper can be seen in Fig. 2(a). The specific steps are shown in Eqs. (1–6). The difference between 3PB and 2PB is if the oxygen ions enter the interior of the electroactive materials. Regarding the reaction mechanism, Eq. (3) denotes the limiting step. Hence, Eq. (3) should be focused and other reactions can be ignored. Finally, two oxygen ions, O^{-}_{ad} and O^{-}_{TPB}, determine the amount of oxygen ion reaction on the oxygen reduction electrode. Among them, the concentration of each ion can be calculated by diffusion equation, as shown in Eq. (7).

Table 1 Heat sources and heat sinks in SOFC-KC-RC system

Heat source	Heat sink
Cooler1	Heater1
Cooler2	Boiler
Condenser1	Evaporator
Condenser2	Pre-reformer
Regenerator	

$$\frac{1}{2}O_2 + S \rightarrow O_{ad} \tag{1}$$

$$O_{ad} + e^- \rightarrow O^-_{ad} \tag{2}$$

$$O^-_{ad} \rightarrow O^-_{TPB} \tag{3}$$

$$O^-_{TPB} + e^- \rightarrow V^{\cdot\cdot}_{O,TPB} \rightarrow O^x_O + S \tag{4}$$

$$O^-_{ad} + V^{\cdot\cdot}_{O,LSM} + e^- \rightarrow O^x_{O,LSM} \tag{5}$$

$$O^x_{O,LSM} + V^{\cdot\cdot}_{O,YSZ} \rightarrow O^x_{O,YSZ} + V^{\cdot\cdot}_{O,LSM} \tag{6}$$

$$\varepsilon\frac{\partial\phi}{\partial t} = \nabla\cdot(D^{eff}_{\phi}\nabla\phi) + S_{\phi}, \tag{7}$$

where ϕ refers to the species concentration. ε refers to the volume fraction of the phase (which is taken as 1 for surface species). D_{ϕ} refers to effective diffusivity, and S_{ϕ} refers to the net source term.

Equation (7) represents a series of partial differential equations including quadratic and first-order. The solution ideas are shown below: the implicit Euler method for time marching is obtained by using forward differencing for the time derivative and central differencing for the diffusion terms. During the solution process in PFRs, the solution method used in this paper is based on differentiating the length of PFRs. The detailed solution method refers to literature [24,25]. For each differential unit, the electrochemical reaction and methane reforming reaction are coupled to solute.

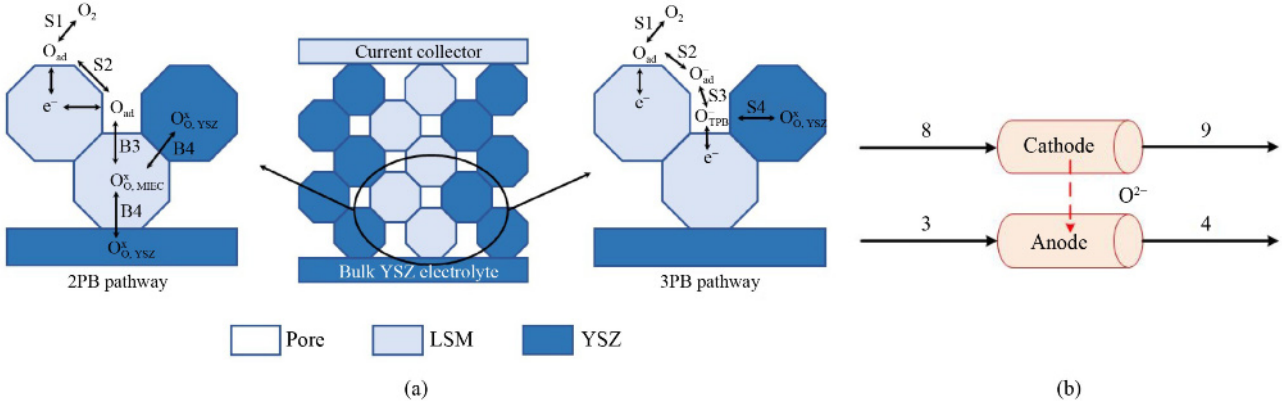

Fig. 2 Flow diagram of SOFC system. (a) Reaction mechanism of the electrode, and (b) the stack simulated by PFRs. Reprinted with permission from Ref. [9], copyright 2014, Elsevier.

2.2 RC subsystem

RC as a thermodynamic system can convert heat into useful work [26]. High-grade temperature waste heat generated by SOFC system is recovered by the top cycle, RC. RC consists of the following components: boiler, turbine, condenser, and pump, which are shown in Fig. 3 [27]. Water absorbs heat in the boiler and is converted to superheated steam [28]. The superheated steam expands in the component turbine1 and the isentropic efficiency of the steam turbine1 is set to be 0.8 [29]. The expanding water from the component Turbine1 goes into the component condenser1. The component condenser1 pressure is similar to component turbine1. The liquid water from the condenser1 is pressurized by the component pump1, and then returned to the component boiler through pump1.

To simulate RC subsystem, the maximum temperature and pressure of superheated steam are set to 1123.15 K and the critical pressure (220.6 bar), respectively [30,31], and it is assumed that the pressure drops of all components except pump and turbine are zero. The property method STEAM-TA is used for RC. In simulating process, a stream is usually divided into several sub-streams because the working fluids of the RC undergo a phase change. These sub-streams in the component boiler undergo three processes including evaporation, superheating and evaporation. Hence, in order to simulate these processes, three heaters are used.

Likewise, other process streams through component condenser1 also involve phase change including cooling and condensing. Therefore, it should be split up into two sub-streams. The hot/cold identity of the stream is identified by the vaporization fraction in the component condenser1. If the stream (S3) is a mixture of gas and liquid, it can be condensed into liquid directly. In the event that it is gaseous, it will be cooled before it is condensed into liquid.

The modeling of RC should be satisfied with the following constraints shown in Eqs. (8–10). Q refers to vaporization fraction, T refers to temperature and P refers to pressure. Equation (8) guarantees that the RC system's lowest temperature is greater than the surrounding air temperature. Equation (9) makes sure that the RC turbine's inlet pressure is larger than its exit pressure. The turbine's minimum allowable steam content is indicated by Eq. (10) [32].

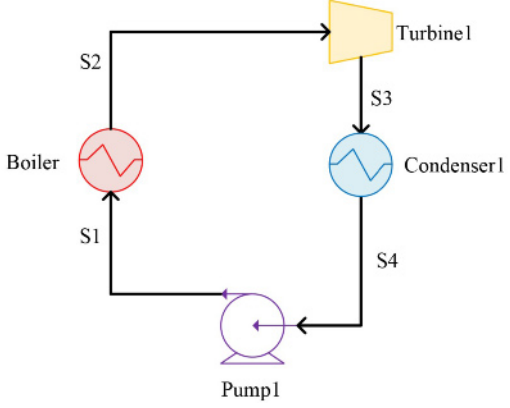

Fig. 3 Schematic diagram of RC subsystem.

$$T_{S4} > 10 + 293.15, \tag{8}$$

$$P_{S3} < P_{S2}, \tag{9}$$

$$0.9 < Q_{S3} < 1. \tag{10}$$

2.3 KC subsystem

KC is a promising heat-to-power technology in low-grad temperature [33]. It recovers low-grad temperature waste heat of RC and SOFC systems, serving as a bottom cycle. The following units are included in KC: mixer, condenser, pump, evaporator, separator, regenerator preheater, valve and turbine, as shown in Fig. 4 [34]. As for the working fluid, the major difference between KC and RC is that the former adopts a mixture of ammonia instead of water. Stream K2 in a high-pressure two-phase mode, enters the component separator for separation to poor solution and rich vapor of the ammonia. The ammonia-lean solution K5 flows to component regenerator for temperature reduction, and then passes through component valve to depressurize. Ammonia-rich steam K3 enters the component turbine2 to generate power. Then these two streams are mixed and enter the component condenser2. Finally, outflow from the component condenser2 pumps to the evaporator. The property method REFPROP is used for KC [35].

Similar to RC, there are phase changes involved in the stream K2 in the component evaporator so it is necessary to decompose it into two sub-streams. The following limitations should be considered, as the assumptions of KC and RC are consistent with each other.

$$0.9 < Q_{K4} < 1, \tag{11}$$

$$0 < Q_{K2} < 1, \tag{12}$$

$$T_{K9} > 10 + 293.15, \tag{13}$$

$$P_{K4} < P_{K3}, \tag{14}$$

where Q stands for vaporization fraction. Equation (12) guarantees the stream that enters the separator in KC subsystem is a mixture of liquid and gas. The remaining constrained conditions are same as those of RC.

3 Model equations

In this section, the mathematical formulations derived from the novel integrated energy system are presented.

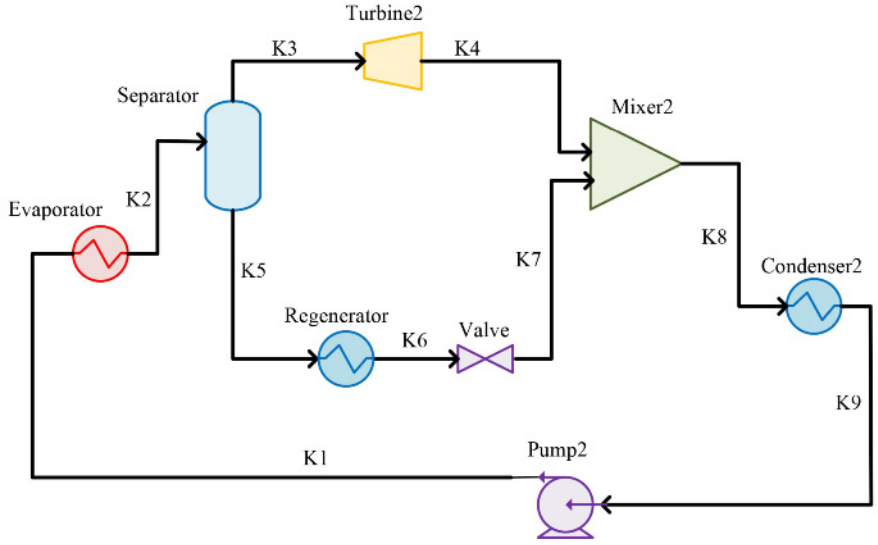

Fig. 4 Schematic diagram of KC subsystem.

The nomenclature and mathematical representations employed in this paper generally follow the forms used in our previous work [22]. Some of the equations and constraints are similarly to those previously proposed. Therefore, more detailed comments are addressed mainly to the model additions and modifications.

3.1 Calculation of voltage and current density

The net output power W_{Stack} of the component stack can be calculated as:

$$W_{\text{Stack}} = i \cdot s \cdot V_{\text{c}}, \tag{15}$$

where s (m^2) stands for surface area. i ($\text{A}\cdot\text{m}^{-2}$) stands for current density. V_{c} (V) stands for the actual voltage of the component stack and it can be deduced as:

$$V_{\text{c}} = V_{\text{R}} - V_{\text{loss}}, \tag{16}$$

$$V_{\text{loss}} = V_{\text{ohm}} + V_{\text{act}} + V_{\text{con}}, \tag{17}$$

where V_{R}, V_{con}, V_{act}, V_{ohm} (V) stand for the cell ideal reversible voltage, the concentration losses, the activation losses and the ohmic losses, respectively. The formulae and corresponding parameters provided by the literature [36] could be used to calculate these variables.

3.2 An enhanced Duran-Grossmann (D-G) model based on stochastic optimization

An enhanced D-G model offers an effective way to tackle the issue of taking heat integration and process optimization into account at the same time. The precise computation formulae are below [37]:

$$\text{QSOA}(x)^{\text{p}} = \sum_{i\in I} FCp_i \left[\max\left\{0, T_i^{\text{in}} - (T^{\text{p}} + \Delta T)\right\} - \max\left\{0, T_i^{\text{out}} - (T^{\text{p}} + \Delta T)\right\}\right], \tag{18}$$

$$\text{QSIA}(x)^{\text{p}} = \sum_{i\in J} FCp_j \left[\max\left\{0, T_j^{\text{out}} - (T^{\text{p}} + \Delta T)\right\} - \max\left\{0, T_j^{\text{in}} - (T^{\text{p}} + \Delta T)\right\}\right], \tag{19}$$

$$Q(x) = \text{QSOA}(x)^{\text{p}} - \text{QSIA}(x)^{\text{p}}, \tag{20}$$

where QSOA and QSIA stand for the heat load of hot and cold stream respectively. T_i^{in} and T_j^{out} stand for the inlet and outlet temperature respectively. FCp_i stands for heat capacity flowrate. ΔT stands for the minimum approach temperature for heat transmission and is set to 10 K. T^{p} stands for pinch point temperature and is descried as:

$$T^{\text{p}} = T_i^{\text{in}} - \frac{\Delta T}{2}, \tag{21}$$

$$T^{\text{p}} = T_j^{\text{out}} - \frac{\Delta T}{2}. \tag{22}$$

However, in the actual solution, a great deal of unknown variables appeared. Therefore, a stochastic optimization approach is adopted to solve these unknown variables. The genetic algorithm (GA) approach is a stochastic optimization method that searches for solutions from random populations. Since GA is an effective algorithm for finding global optimum, a two-layer GA is chosen to solve the problem with the goal of achieving the maximum power generation in the process of solving. In solving process, the GA tool in the optimization toolbox of MATLAB is used. The specific optimization procedure is displayed in Fig. 5.

In the inner layer optimization, the parameters related to the PFRs are given. dL to solve the key is an infinitesimal vector element. After the parameters are set, a volume differential unit with a length of dL and a diameter of the inner diameter of the PFR tube is selected. Then the mole fraction of each substance is solved based on the equation of state SRK. When the

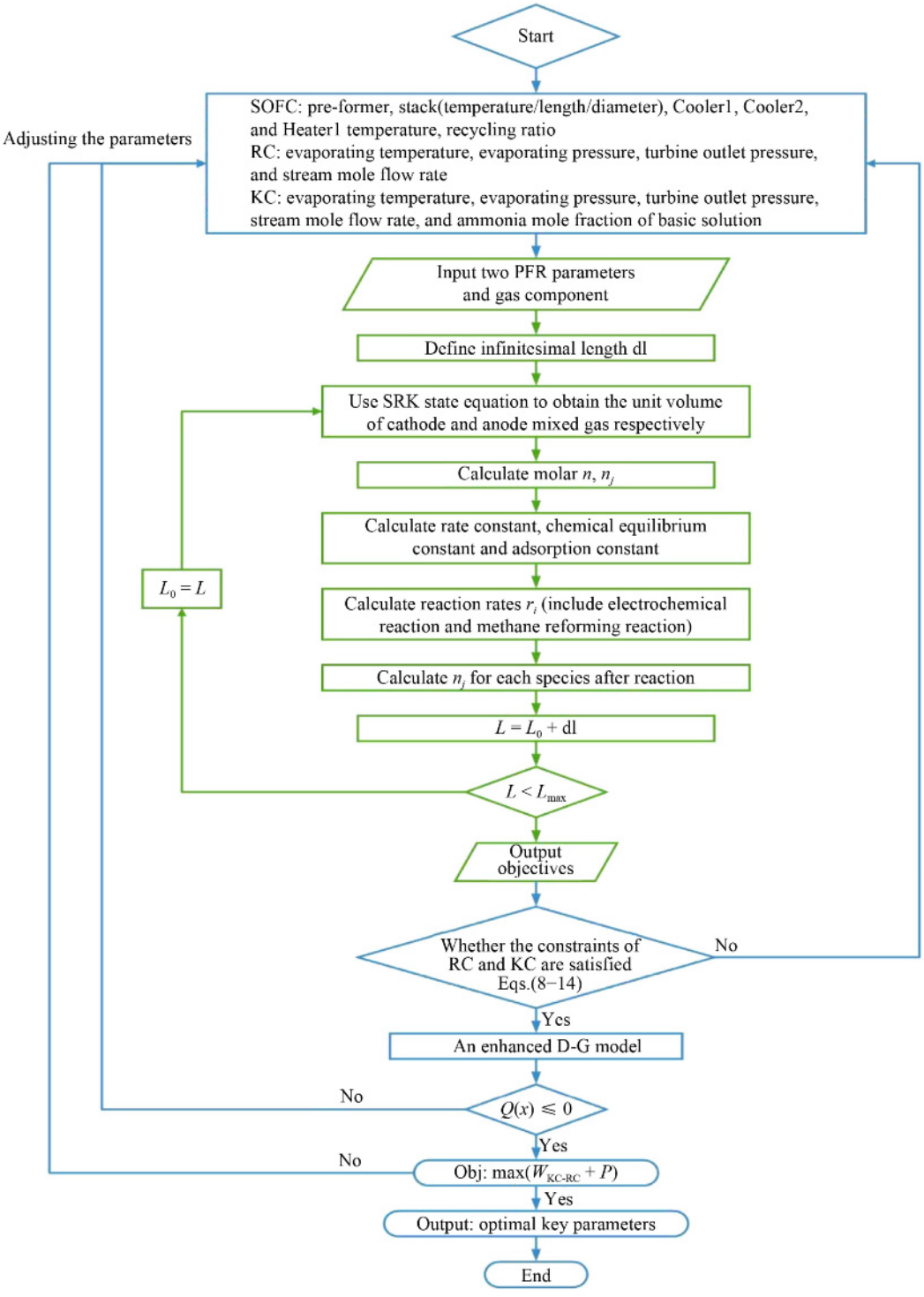

Fig. 5 GA-based optimization procedure for SOFC-KC-RC design.

length of PFR is greater than the set value, exit the loop and output the calculation solution. Regarding the outer layer optimization in the established Aspen-MATLAB interaction platform, one of the streams as the circulating streams needs to be iterated. Wegstein method is used during iteration. When convergence is reached, the iteration ends.

4 Results and discussion

4.1 Sequential optimization

The sequential optimization based on rigorous kinetics model is conducted to optimize the operating conditions of SOFC system. On the basis of the SOFC system

operating conditions, KC-RC system structure and parameters are optimized to make the power generation of KC-RC system maximized. KC-RC mainly recovers multi-grade waste heat from heater1, per-reformer, cooler1 and cooler2 in SOFC systems. For these components that are capable of performing waste heat recovery, their heat load can be calculated from the enthalpy value of their intake and output streams.

When optimizing SOFC systems individually, thermal utilities are not needed for SOFC system. The optimization result can be seen in Table 2. After the SOFC system is optimized by the extended D-G model based on stochastic optimization, KC and RC are calculated on the obtained operating conditions of SOFC system. The hot/cold identity of streams 1-2 and 2-3 in pre-reformer and heater1 should be determined according to the heat load, which should be paid special attention to. MATLAB is used to code the corresponding constraints.

The specific iterative process of stochastic optimization is displayed in Fig. 6. Up to the 60th generation, the output power of KC-RC system is gradually smooth and the optimization solution can be obtained. The optimization results of KC-RC system in this case are shown in Table 3.

The hot and cold composite curves for SOFC-KC-RC are drawn in Fig. 7 according to the results of sequential optimization. Figure 7 shows that there are two pinch points in SOFC-KC-RC system, approximately at 332 and 424 K. Between the cold stream of evaporator in KC and the hot stream of condenser2 is where the first pinch point is situated. The location of the first pinch point is similar to the waste heat based on thermodynamics model. Then between the cold stream of heater1 and the hot stream of the condenser is where the pinch point is.

4.2 Simultaneous optimization

Because SOFC systems are considered separately from KC-RC in sequential optimization, it is basically impossible to guarantee the overall output power of the SOFC-KC-RC system to reach the maximum. Hence, simultaneous optimization is implemented, in which the output power of SOFC, KC and RC are considered to be the objective function. In the simultaneous optimization, the primary operating conditions of each component and the heat-transfer matched in the SOFC-KC-RC are optimized concurrently. The variation range of operating parameters in the SOFC system during stochastic optimization is revealed in Table 4. The temperature of component cooler2 is set to 313.5 K, and it can be seen in literature [22]. Using GA, 14 variables—including 9

Table 2 Specific operating conditions of the SOFC system in sequential optimization

Parameter	Value
Heater1 inlet temperature/K	298.2
Heater1 outlet temperature/K	907.7
Cooler1 inlet temperature/K	1118.9
Cooler1 outlet temperature/K	1236.4
Cooler2 inlet temperature/K	1496.9
Cooler2 outlet temperature/K	313.2
Stack temperature/K	1271.7
Pre-reformer temperature/K	966.3
Stack PFR diameter/m	0.149
Stack PFR length/m	0.299
Amount of catalyst	491.0
Recycling ratio	0.686

Table 3 Results of sequential optimization for KC and RC

Parameters	Value
KC evaporating temperature/K	417.53
KC evaporating pressure/bar	43.82
KC turbine outlet pressure/bar	6.67
KC stream mole flow rate/(kmol·h^{-1})	86.47
KC power/kW	34.98
RC evaporating temperature/K	1270.10
RC evaporating pressure/bar	220.25
RC turbine outlet pressure/bar	5.24
RC stream mole flow rate/(kmol·h^{-1})	23.90
RC power/kW	138.63
Ammonia mole fraction of basic solution	0.66
Stack power/kW	146.95
Total power/kW	320.56

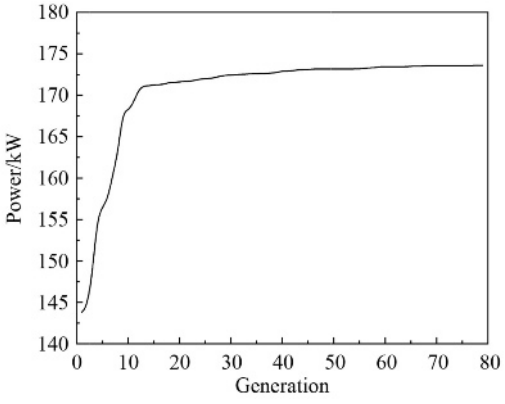

Fig. 6 GA solving process for sequential optimization.

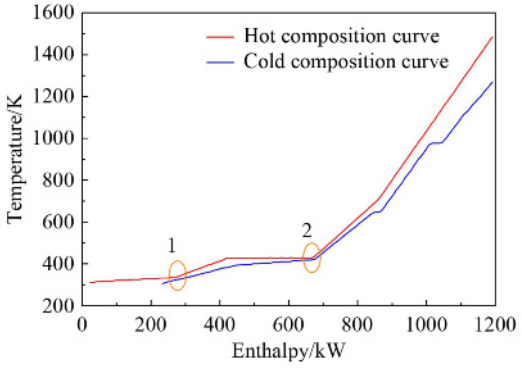

Fig. 7 Hot and cold composite curves for SOFC-KC-RC in sequential optimization.

Table 4 Ranges of critical optimization variables in simultaneous optimization

Components	Optimization interval
Pre-former temperature	793.15–973.15 K
Stack temperature	873.15–1273.15 K
Stack PFR diameter	0.1–0.3 m
Stack PFR length	0.1–0.3 m
Recycling ratio	0.6–0.8
Heater1 outlet temperature	473.15–1273.15 K
Heater2 outlet temperature	373.15–1273.15 K

cycle power generation parameters and 5 process parameters—are optimized, much like in sequential optimization.

The calculation result of simultaneous optimization is shown in Fig. 8, from which it can be seen that the optimization curve is not as flat as in the literature [22]. This is due to the need to iterate the kinetics model of SOFC system. The iterate in SOFC system requires a lot of computation and is complex. Hence, its calculation shows such a result. The maximum overall output power is 415.0 kW, of which 282.67 kW is generated by KC-RC and 132.37 kW is derived from the SOFC system. The overall output power of SOFC-KC-RC system has been increased by 22.92% compared with sequential optimization. Although the SOFC system electric power drops from 146.95 to 132.37 kW, KC-RC power generation increases by 62.82%. This calculation result is not only different from the sequential optimization, but also different from the simultaneous optimization based on the thermodynamic model. The largest difference compared to simultaneous optimization based on thermodynamic models is the differences in modeling methods for SOFC systems. This difference leads to a different energy recovery bottleneck.

The hot and cold composite curves of SOFC-KC-RC are shown in Fig. 9. It is clearly shown that there is no pinch point. The appearance of a pinch point represents the energy consumption bottleneck, and the absence of a pinch point in simultaneous optimization indicates that the energy consumption bottleneck has been broken.

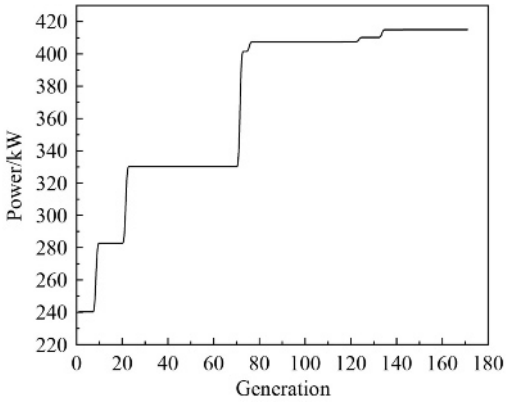

Fig. 8 GA solving process for simultaneous optimization.

Besides, Fig. 9 illustrates that, in comparison to sequential optimization, simultaneous optimization results in a higher stream temperature level.

The values of the parameters of the SOFC-KC-RC system in the above calculation results, which change slightly from sequential optimization, are displayed in Table 5. For the component stack, the temperature and size decrease but the amount of catalyst increases. In the RC system, the evaporation temperature and mole flow rate increase because of the increased waste heat recovery from SOFC systems. The pressure of the RC turbine and the component condenser1 are comparable. Hence, turbine pressure of the RC system needs to be balanced between the power produced and the waste heat of condenser1. Finally, the pressure of component turbine1 decreases. The increased stream flow of RC is caused by the

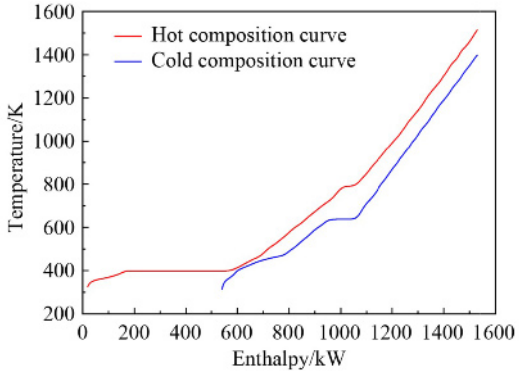

Fig. 9 Hot and cold composite curves of SOFC-KC-RC in simultaneous optimization.

Table 5 Results of simultaneous optimization for SOFC-KC-RC

Parameters	Value
KC evaporating temperature/K	478.78
KC evaporating pressure/bar	45.81
KC turbine outlet pressure/bar	6.80
RC evaporating temperature/K	1403.10
RC evaporating pressure/bar	205.48
RC turbine outlet pressure/bar	3.01
KC stream mole flow rate/(kmol·h^{-1})	31.78
RC stream mole flow rate/(kmol·h^{-1})	38.47
Heater1 inlet temperature/K	298.15
Heater1 outlet temperature/K	385.84
Cooler1 inlet temperature/K	1044.20
Cooler1 outlet temperature/K	697.70
Pre-reformer temperature/K	794.64
Stack temperature/K	1203.24
Stack PFR length/m	0.28
Stack PFR diameter/m	0.11
Amount of catalyst/g	511.07
Recycling ratio	0.60
Ammonia mole fraction of basic solution	0.32
Stack power/kW	273.08
KC power/kW	132.37
RC power/kW	9.59
Total power/kW	415.04

increased waste heat in SOFC system. The evaporation temperature of KC rises as a result of an increase in the overall waste heat of RC and SOFC system.

The earlier work just used a conversion reactor to simulate the cathode side of component stack and failed to account for reaction kinetics. In this work, this deficiency is solved by introducing electrode microscopic reaction kinetics. Hence, the simulation of the SOFC system is improved and the results of waste heat recovery based on this model are also upgraded. Comparing the calculation results in this work with those in our previous work [22], it is found that the results in this work indicates a 10.8% increase in power generation with a higher energy utilization efficiency.

5 Conclusions

In this work, an upgraded integrated energy system SOFC-KC-RC is developed for multiple waste heat recovery. The proposed system combines kinetic model-based SOFC with thermal cycles to maximize the power generation, by arranging KC as a bottom cycle and RC as a top cycle. In developing the novel kinetic model of SOFC, two PFRs serve as the simulator of anode and cathode of the component stack. In PFRs, the length of PFR is differentiated and the mole fraction of each substance is solved according to the methane reforming kinetic equation and electrode microscopic reaction kinetic equation in every differential unit. Regarding waste heat recovery, KC and RC are used to recover high-temperature waste heat and low-temperature waste heat of SOFC system respectively, where the extended D-G model based on stochastic optimization is used to sequentially and simultaneously heat-transfer structures and optimize operating conditions for maximum power generation. As far as we are aware, it is the first stochastic method for the optimal design of kinetics-based SOFC combined thermal cycle to generate power. Major concluding remarks introduced by this work include: (1) According to the result of sequential optimization, the SOFC subsystem power is 146.95 kW and the KC-RC power generation is 173.61 kW on condition that the operating parameters of the SOFC subsystem are set. (2) Both KC-RC structures and the SOFC subsystem parameters are optimized concurrently in simultaneous optimization. The outcome demonstrates that the power generated by SOFC-KC-RC is 415.04 kW, and the overall output power increases by 29.5% than that obtained by sequential optimization. (3) Further in comparison with the open solutions reported by a thermodynamic model in our previous work, this work indicates a 10.8% increase in power generation, which demonstrates that the developed system is more promising in power generation with a higher energy utilization efficiency than that in the previous studies.

While our focus is on exploring the integration SOFC with thermal cycle in a synergistic manner to improve the total power generation and computational performance, the number of devices and the equipment investment cost are not considered. This simplified consideration is to lessen the restrictions and nonlinearity. Estimating heat transfer regions and designing every device for a more detailed energy integrated system should be the focus of future effort.

Acknowledgements This work was financially supported by the financial support provided by the National Natural Science Foundation of China (Grant Nos. 22008023, and 22178045) and Fundamental Research Funds for the Central Universities (Grant No. DUT21RC(3)109).

Competing interests The authors declared that they have no competing interests.

Nomenclature

Notations in formulation

D_ϕ	effective diffusivity
i	current density
L	length
n	molar flow rate
P	pressure/percolation probability
Q	vaporizing fraction
QSOA	heat load of hot streams
QSIA	heat load of cold streams
s	surface area
S_ϕ	net source term
T	temperature
V_{C}	produced cell voltage
V_{con}	concentration overvoltage
V_{loss}	voltage loss
V_{ohm}	ohmic overvoltage
V_{act}	activation loss
V_{R}	ideal reversible voltage
W_{stack}	net power generation
ΔT	minimum heat transfer approach temperature
ε	volume fraction
ϕ	species concentration

Subscript

i	hot streams
j	cold streams

Superscript

in	inlet
out	outlet
p	pinch candidate

References

1. Ng K H, Rahman H A, Somalu M R. Review: enhancement of composite anode materials for low-temperature solid oxide fuels. International Journal of Hydrogen Energy, 2019, 44(58): 30692–30704
2. Lu H T, Li W, Miandoab E S, Kanehashi S, Hu G. The opportunity of membrane technology for hydrogen purification in the power to hydrogen (P_2H) roadmap: a review. Frontiers of Chemical Science and Engineering, 2021, 15(3): 464–482
3. Konysheva E Y. Reduction of CeO_2 in composites with transition metal complex oxides under hydrogen containing atmosphere and its correlation with catalytic activity. Frontiers of Chemical Science and Engineering, 2013, 7(3): 249–261
4. Manishanma S, Dutta A. Synthesis and characterization of nickel doped LSM as possible cathode materials for LT-SOFC application. Materials Chemistry and Physics, 2023, 297: 127438
5. Park C, Kim Y H, Jeong H, Won B, Jeon H, Myung J. Development of robust YSZ thin-film electrolyte by RF sputtering and anode support design for stable IT-SOFC. Ceramics International, 2023, 49(20): 32953–32961
6. Asghar M I, Lepikko S, Patakangas J, Halme J, Lund P D. Comparative analysis of ceramic-carbonate nanocomposite fuel cells using composite GDC/NLC electrolyte with different perovskite structured cathode materials. Frontiers of Chemical Science and Engineering, 2018, 12(1): 162–173
7. Lim Y, Park J, Lee H, Ku M, Kim Y B. Rapid fabrication of lanthanum strontium cobalt ferrite (LSCF) with suppression of LSCF/YSZ chemical side reaction via flash light sintering for SOFCs. Nano Energy, 2021, 90: 106524
8. Chan S H, Chen X J, Khor K A. Cathode micromodel of solid oxide fuel cell. Journal of the Electrochemical Society, 1997, 151: 134–140
9. Pakalapati S, Gerdes K, Finklea H, Gong M, Liu X, Celik I. Micro scale dynamic modeling of LSM/YSZ composite cathodes. Solid State Ionics, 2014, 258: 45–60
10. Yang T, Liu J, Finklea H O, Abernathy H, Hackett G A. Multi-physics simulation of SOFC button cell with multi-step charge transfer model in composite LSM/YSZ cathode. Journal of the Electrochemical Society, 2017, 78: 2699–2709
11. Banerjee A, Deutschmann O. Elementary kinetics of the oxygen reduction reaction on LSM-YSZ composite cathodes. Journal of Catalysis, 2017, 346: 30–49
12. Zhang Y, Wu S, Cui D, Yoon S, Bae Y, Park B, Wu Y, Zhou F, Pan C, Xiao R. Energy and CO_2 emission analysis of a bio-energy with CCS system: biomass gasification-solid oxide fuel cell-mini gas turbine-CO_2 capture. Fuel Processing Technology, 2022, 238: 107476
13. Er-rbib H, Kezibri N, Bouallou C. Performance assessment of a power-to-gas process based on reversible solid oxide cell. Frontiers of Chemical Science and Engineering, 2018, 12(4): 697–707
14. Pianko-Oprych P, Palus M. Simulation of SOFCs based power generation system using Aspen. Polish Journal of Chemical Technology, 2017, 19(4): 8–15
15. Veluswamy G K, Laycock C J, Shah K, Ball A S, Guwy A J, Dinsdale R M. Biohythane as an energy feedstock for solid oxide fuel cells. International Journal of Hydrogen Energy, 2019, 44(51): 27896–27906
16. Milewski J, Szczęśniak A, Szabłowski Ł. A proton conducting solid oxide fuel cell-implementation of the reduced order model in available software and verification based on experimental data. Journal of Power Sources, 2021, 502: 229948
17. Saebea D, Arpornwichanop A, Patcharavorachot Y. Thermodynamic analysis of a proton conducting SOFC integrated system fuelled by different renewable fuels. International Journal of Hydrogen Energy, 2021, 46(20): 11445–11457
18. Xie D, Ling A, Yan D, Jia L, Chi B, Pu J, Li J. A comparative study on the composite cathodes with proton conductor and oxygen ion conductor for proton-conducting solid oxide fuel cell. Electrochimica Acta, 2020, 344: 136143
19. Wang Z, Chen H, Xia R, Han F, Ji Y, Cai W. Energy, exergy and economy (3E) investigation of a SOFC-GT-ORC waste heat recovery system for green power ships. Thermal Science and Engineering Progress, 2022, 32: 101342
20. Chitgar N, Moghimi M. Design and evaluation of a novel multi-generation system based on SOFC-GT for electricity, fresh water and hydrogen production. Energy, 2020, 197: 117162
21. Tera I, Zhang S, Liu G. A conceptual hydrogen, heat and power polygeneration system based on biomass gasification, SOFC and waste heat recovery units: energy, exergy, economic and emergy (4E) assessment. Energy, 2024, 295: 131015
22. Song M, Zhuang Y, Zhang L, Li W, Du J, Shen S. Thermodynamic performance assessment of SOFC-RC-KC system for multiple waste heat recovery. Energy Conversion and Management, 2021, 245: 114579
23. Xu J, Froment G F. Methane steam reforming, methanation and water-gas shift: 1. Intrinsic kinetics. AIChE Journal, 1989, 35(1): 88–96
24. Li W, Zhuang Y, Liu L, Zhang L, Du J. Process evaluation and optimization of methanol production from shale gas based on kinetics modeling. Journal of Cleaner Production, 2020, 274: 123153
25. Verda V, Quaglia M C. Solid oxide fuel cell systems for distributed power generation and cogeneration. International Journal of Hydrogen Energy, 2008, 33(8): 2087–2096
26. Khater A M, Soliman A, Ahmed T S, Ismail I M. Power generation in white cement plants from waste heat recovery using steam-organic combined Rankine cycle. Case Studies in Chemical and Environmental Engineering, 2021, 4: 100138
27. Yue T, Lior N. Thermodynamic analysis of hybrid Rankine cycles using multiple heat sources of different temperatures. Applied Energy, 2018, 222: 564–583
28. Zhang H, Li M, Feng Y, Xi H, Hung T. Assessment and working fluid comparison of steam Rankine cycle-Organic Rankine cycle combined system for severe cold territories. Case Studies in Thermal Engineering, 2021, 28: 101601
29. Zhu S, Deng K, Qu S. Energy and exergy analyses of a bottoming Rankine cycle for engine exhaust heat recovery. Energy, 2013, 58: 448–457
30. Nazari N, Heidarnejad P, Porkhial S. Multi-objective optimization

of a combined steam-Organic Rankine cycle based on exergy and exergo-economic analysis for waste heat recovery application. Energy Conversion and Management, 2016, 127: 366–379

31. Mashadi B, Kakaee A, Horestani A J. Low-temperature Rankine cycle to increase waste heat recovery from the internal combustion engine cooling system. Energy Conversion and Management, 2019, 182: 451–460
32. Köse Ö, Koç Y, Yağlı H. Performance improvement of the bottoming steam Rankine cycle (SRC) and Organic Rankine cycle (ORC) systems for a triple combined system using gas turbine (GT) as topping cycle. Energy Conversion and Management, 2020, 211: 112745
33. Cheng Z, Wang J, Yang P, Wang Y, Chen G, Zhao P, Dai Y. Comparison of control strategies and dynamic behaviour analysis of a Kalina cycle driven by a low-grade heat source. Energy, 2022, 242: 122958
34. Singh O K. Application of Kalina cycle for augmenting performance of bagasse-fired cogeneration plant of sugar industry. Fuel, 2020, 267: 117176
35. Wang Y, Tang Q, Wang M, Feng X. Thermodynamic performance comparison between ORC and Kalina cycles for multi-stream waste heat recovery. Energy Conversion and Management, 2017, 143: 482–492
36. Fallah M, Mahmoudi S M S, Yari M. Advanced exergy analysis for an anode gas recirculation solid oxide fuel cell. Energy, 2017, 141: 1097–1112
37. Yu H, Eason J, Biegler L T, Feng X. Process integration and superstructure optimization of Organic Rankine cycles (ORCs) with heat exchanger network synthesis. Computers & Chemical Engineering, 2017, 107: 257–270